Thin films of CsPbBr$_3$ nanocrystals on scintillating wafers

Jan Král [1], Kateřina Děcká [1,5], Fiammetta Pagano[3,4], Nicolaus Kratochwil [3], Vladimir Babin [5], František Hájek [2,5], Eva Mihóková [2,5], Etiennette Auffray [3], Václav Čuba [1]

[1]Department of Nuclear Chemistry, Faculty of Nuclear Sciences and Physical Engineering, Czech Technical University in Prague
[2]Department of Solid State Engineering, Faculty of Nuclear Sciences and Physical Engineering, Czech Technical University in Prague
[3]CERN, Geneva, Switzerland
[4]University of Milano-Bicocca, Italy
[5]Institute of Physics of the Czech Academy of Sciences
kralja13@fjfi.cvut.cz

Abstract

There is a rising demand for new detectors with ultra-fast timing for the use of Time-Of-Flight measurements in medical imaging and high-energy physics. One way of tackling this challenge is a composite material of bulk inorganic scintillators with nanoscintillators exhibiting quantum confinement effect. In this work, thin films of CsPbBr$_3$ nanocrystals were prepared on various substrates and their radioluminescent and timing properties were tested. Enhancement in radioluminescence intensity and addition of ultrafast decay components was observed by applying CsPbBr$_3$ thin film on scintillating wafers. Significant improvements in detector time resolution of composite materials in comparison with pure inorganic scintillating crystals were observed.

Keywords: Cesium lead bromide; Nanocrystals; Scintillation; Thin films; Fast timing.

Introduction

CsPbBr$_3$ nanocrystals (NC) are new materials that possess exciting properties thanks to the so-called defect tolerant perovskite structure and quantum confinement effect [1]. These provide CsPbBr$_3$ NC with their very high quantum efficiencies (close to 100%), fast decay times and narrow tunable emission peak which makes them an interesting candidate for many applications from LED, and luminescent solar concentrators to radiation detection [2].

In radiation detection, the need for ultra-fast timing has emerged for applying Time-of-Flight (TOF) measurements, especially in medical imaging and high-energy physics [3]. TOF measurement is already established in positron emission tomography, but would greatly profit from further improvements in the timing capabilities of used detectors to achieve real-time image reconstruction [4]. Ultra-fast detectors could also be applied to introduce TOF measurements into X-ray photon detection to discriminate Compton and Rayleigh scatter contribution and therefore enhance the contrast-to-noise ratio and/or reduce the X-ray exposure dose in computed tomography [5].

Inorganic scintillating bulk crystals used in these fields as modern LYSO:Ce do not possess a sufficiently fast scintillating response for demanded timing performance and new detector materials are needed. One way of tackling the challenge of ultra-fast timing is the preparation of composite materials, combining the stopping power of inorganic scintillators

with the ultra-fast luminescence of nanoparticles exhibiting the quantum confinement effect [6].

In this work, we prepared thin films of $CsPbBr_3$ NC on various scintillating wafers. Radioluminiscence properties and decay times of composites were characterised and detector time resolution (DTR) values under X-ray excitation were measured. DTR measurement quantifies the timing capabilities of the sample by measuring the time delay between the trigger signal of the excitation pulse and the signal from the silicon photomultiplier tube (SiPM). DTR is similar to coincidence time resolution used in PET but is measured with lower excitation energy in order to better characterize samples with lower stopping power.

Experimental section

$CsPbBr_3$ NC synthesis and preparation of thin films

$CsPbBr_3$ NC were prepared on a Schlenk line using a Hot-Injection (HI) method presented by Protesescu et al. [7], but the original synthesis was modified. Specifically, in the preparation of caesium oleate, the oleic acid (OA) to caesium ratio in the reaction mixture was increased to 5:1 according to Lu et. al [8], amount of OA in the next steps was then adjusted to ratios used in the original synthesis.

The synthesis was followed by a ligand exchange reaction replacing OA and oleylammonium ligands with didodecyldimethylammonium bromide. Details of the whole synthesis can be found in Děcká [9]. The final solution was obtained by dispersing NC in toluene.

For thin film preparation as-synthesized solution with a concentration of approximately 50 mg/ml was used. Two deposition methods of the solution onto the wafer were used. Samples for the characterization of radioluminescent properties were prepared by a spin-coating procedure. The solution was repeatedly deposited on a stationary wafer followed by rotation at 2000 rpm for 1 min. Samples for DTR measurement were obtained by drop-casting the $CsPbBr_3$ solution on the wafer as they were too small for the spin-coater. As wafers, LYSO ($Lu_1.8Y_0.2SiO_5$) crystal doped with Ce and GGAG ($Gd_3Ga_{2.7}Al_{2.3}O_{12}$) crystal doped with Ce and Mg were used in form of 3×3 mm^2 plates with a thickness of 0.2 mm.

Characterization

Radioluminescence (RL) spectra were collected using a 5000M spectrofluorometer (Horiba Jobin Yvon) with a monochromator and TBX-04 (IBH Scotland) photodetector, the excitation source was a Seifert X-ray tube (40 kV, 15 mA). RL decay curves were collected using the hybrid picosecond photon detector HPPD-860 and Fluorohub unit (Horiba Scientific). Samples were excited by the picosecond (ps) X-ray tube N5084 from Hamamatsu, operating at 40 kV. The X-ray tube was driven by the ps light pulser (Hamamatsu) equipped with a laser diode operating at 405 nm. The instrumental response function FWHM of the setup is about 76 ps.

For DTR measurement samples were glued from the wafer side with Meltmount on SiPMs from Hamamatsu (S13360 3050PE, 9V above breakdown) and excited by x-ray with a median energy of 9 keV. For the analysis, all events independent of the deposited energy were considered and no correction from the timing jitter of the setup (pulse width of the laser, time response of the X-ray tube, together $\approx$ 100 ps full width at half maximum

- FWHM) was performed. The detector time resolution (DTR) was calculated as the FWHM of the time delay distribution with respect to the external trigger.

Results and Discussion

Spin-coated CsPbBr$_3$ thin films were prepared on wafers from LYSO:Ce (LYSO) and GGAG:Ce,Mg (GGAG) scintillating bulk crystals. Features of RL spectra will be presented on the GGAG sample because it showed the more promising results, the same effects discussed for the GGAG sample are present in the LYSO sample as well, but produce different results.

Radioluminiscence spectra of pure CsPbBr$_3$ NC thin film on non-scintillating glass wafer, GGAG wafer and composite sample GGAG+CsPbBr$_3$ are in Figure 1(a). There are three main features, which can be seen in spectra. First, RL of the composite was suppressed under 520 nm, which can be ascribed to absorption of GGAG wafer RL by CsPbBr$_3$ thin film (as demonstrated by an overlap of CsPbBr$_3$ absorption spectra and pure GGAG emission in Figure 1(a)). A second interesting feature of spectra is a region of longer wavelengths, where GGAG wafer RL intensity in the composite is enhanced compared to pure GGAG wafer. This was attributed to the cracked character of thin film as confirmed by SEM (Figure 1(b)) and improved light collection thanks to light scattering on the film. The last feature of spectra is the significant enhancement of composite RL compared to pure GGAG in the green region, where CePbBr$_3$ NC emit. This feature is most probably a combination of both above-mentioned effects: GGAG wafer RL intensity is enhanced due to increased light scattering and CsPbBr$_3$ thin film emission is increased due to remission of absorbed GGAG light.

For LYSO with CsPbBr$_3$ thin film, worse results compared to GGAA composite were obtained mainly due to degradation of overall RL intensity of the sample. Most of the RL intensity of the LYSO wafer in the composite sample was suppressed by CsPbBr$_3$ layer because of a larger overlap of scintillating wafer emission spectral position and CsPbBr$_3$ absorption and enhancement of CsPbBr$_3$ emission by absorbing this light was limited. In future research, the compatibility of scintillating wafer and NC can be further optimized by changing the optical properties of nanoparticles. Absorption and emission of perovskite NC can be moved to the blue spectral region by preparation of CsPb(Br/Cl)$_3$ [10] mixed perovskites or pure CsPbCl$_3$ [7].

RL decay curves for CsPbBr$_3$ thin film, pure GGAG and composite GGAG + CsPbBr$_3$ sample are in Figure 1(c),(d) and results are summarized in Table 1. The measured RL decay curve of pure CsPbBr$_3$ NC thin film on a glass wafer shows ultrafast luminescence of CsPbBr$_3$ NC with two subnanosecond decay components. The same subnanosecond components of CsPbBr$_3$ decay are also present in the composite sample in contrast to pure GGAG. The long components of GGAG in the composite sample are not precisely determined, because the measurement was done in a short time window to resolve ultrafast CsPbBr$_3$ components. The addition of ultrafast subnanosecond decay components to the RL response of scintillating wafers was also observed in LYSO composite sample. These results demonstrate that applying CsPbBr$_3$ thin films on the scintillating crystal adds fast decay components to the sample's response.
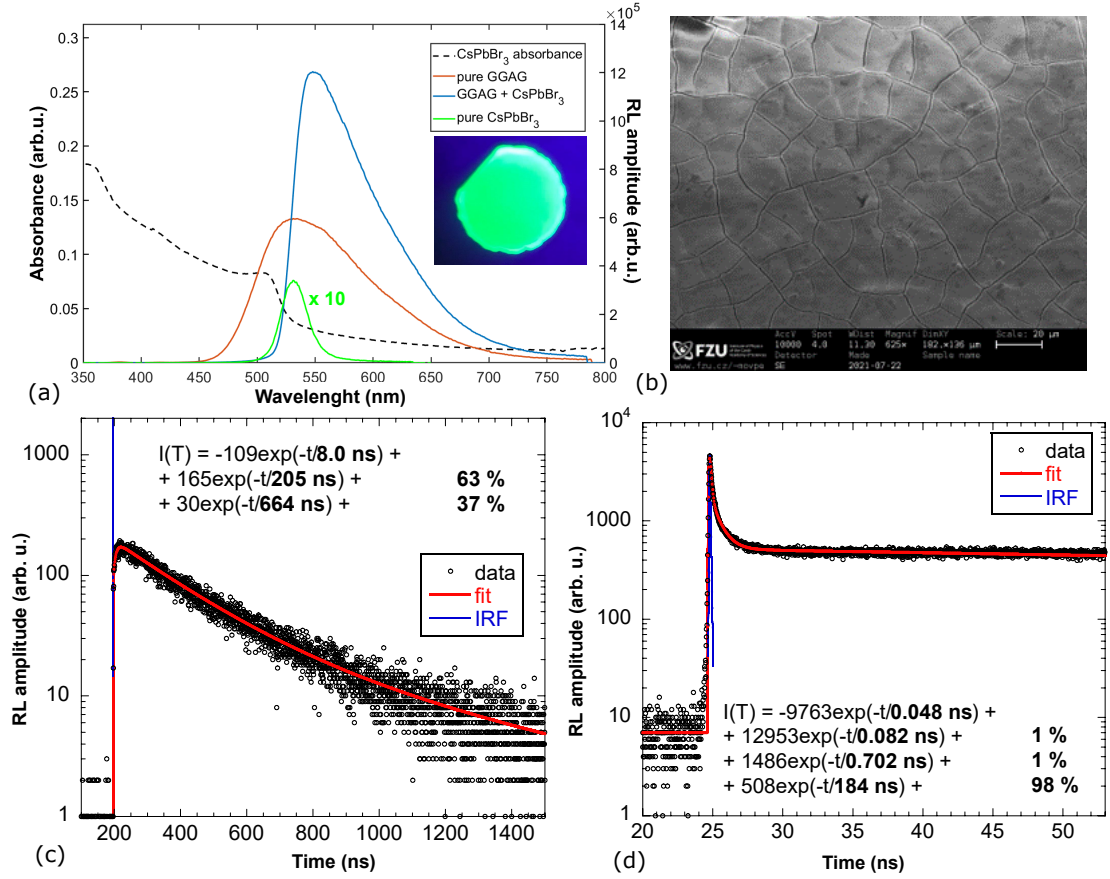
Figure 1: (a) RL spectra of pure GGAG (red line), CsPbBr$_3$ thin film on glass (green line), composite sample GGAG+CsPbBr$_3$ (blue line) and CsPbBr$_3$ absorption (black dotted line), inset: the photography of composite sample under UV excitation, (b) SEM micrograph of CsPbBr$_3$ thin film on GGAG wafer, (c) decay curve of GGAG sample with fit measured in a long time window, (d) decay curve of GGAG+CsPbBr$_3$ composite sample with fit measured in a short time window.

Table 1: Radioluminiscnce decay components τ_1-τ_4 measured for CsPbBr$_3$ NC thin film, GGAG and composite sample.

	CsPbBr$_3$		GGAG		GGAG + CsPbBr$_3$	
τ_1	45 ps	19%	-	-	80 ps	1%
τ_2	350 ps	34%	-	-	700 ps	1%
τ_3	2 ns	30%	200 ns	63%	long	98%
τ_4	11 ns	17%	660 ns	37%	-	-

In the next step, DTR values of prepared composites were measured to examine if the addition of fast decay components of CsPbBr$_3$ can improve the timing performance of scintillating crystals.

Measured coincidence time delay histograms and DTR values for composites, pure inorganic scintillators and pure CsPbBr$_3$ thin film on SiPM are presented in Figure 2. Composite samples exhibit a significant improvement in timing capabilities in comparison

with pure bulk scintillators. Both composite samples achieved similarly low DTR values independent of which scintillating wafer was used, which points to the importance of $CsPbBr_3$ in achieving improved timing. When pure $CsPbBr_3$ thin film on SiPM was measured, the best timing performance (DTR = 226 ± 7 ps) was recorded.

The essential contribution of $CsPbBr_3$ thin film for timing performance was further demonstrated by measurement of the sample in the flipped configuration in which the sample is coupled with SiPM in a way that thin film is located in between the scintillating wafer and SiPM. DTR value similar to pure GGAG was obtained for this flipped sample and no significant difference in response was observed. This is most probably due to all the x-ray radiation being stopped by the scintillating wafer which leads to no excitation of $CsPBBr_3$.

DTR values of $CsPbBr_3$ samples are a twofold improvement in comparison to LYSO crystal (commercially used nowadays in TOF-PET) which shows promising potential and applicability of perovskite materials for fast timing. To compare further, $CsPbBr_3$ samples also achieved slightly better DTR values than measured for fast commercial organic scintillator EJ232 (DTR= 313 ± 10 ps) while promising higher density and stopping power. In future work, routes how to incorporate NC into polymeric matrices should be explored in order to protect NC from a detrimental influence of the environment.
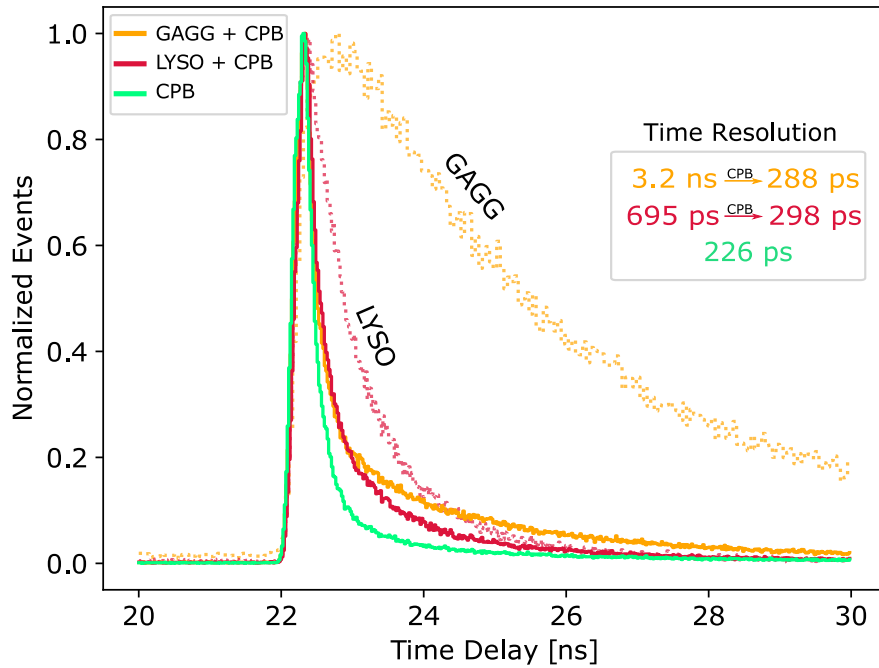

Figure 2: Normalized coincidence time delay distribution without (dotted lines) and with drop-casted CPB (solid lines) on top of inorganic bulk GGAG and LYSO and pure $CsPBBr_3$ thin film.

Conclusions

In this work, we demonstrate the potential of $CsPbBr_3$ NC to significantly improve the timing performance of bulk scintillators. First, we showed that the application of $CsPbBr_3$ thin film can provide ultrafast subnanosecond decay components to inorganic scintillator and depending on scintillator emission spectral position even improve light output. In the next step, it was shown that thin films of $CsPbBr_3$ NC on bulk scintillators significantly improve DTR values under soft X-ray excitation. In future work, routes of NC incorporation into polymeric matrices will be explored. Further, the synergy between NC and bulk scintillators can be optimized by changing NC absorption and emission spectral position.

References

[1] J. Shamsi, et al. Metal Halide Perovskite Nanocrystals: Synthesis, Post-Synthesis Modifications, and Their Optical Properties. *Chemical Reviews* **119**(5): 3296-3348, 2019.

[2] A. Dey, et al. State of the Art and Prospects for Halide Perovskite Nanocrystals. *ACS Nano* **15**(7): 10775-10981, 2021.

[3] C. Dujardin, et al. Needs, Trends, and Advances in Inorganic Scintillators. *IEEE Transactions on Nuclear Science* **65**(8): 1977-1997, 2018.

[4] P. Lecoq, et al. Pushing the Limits in Time-of-Flight PET Imaging. *IEEE Transactions on Radiation and Plasma Medical Sciences* **1**(6): 473-485, 2017.

[5] J. Rossignol, et al. Time-of-flight computed tomography - proof of principle. *IOP Publishing* **65**(8): 085013, 2020.

[6] P. Lecoq, et al. Roadmap toward the 10 ps time-of-flight PET challenge. *IOP Publishing* **65**(21): 21RM01, 2020.

[7] L. Protesescu, et al. Nanocrystals of Cesium Lead Halide Perovskites ($CsPbX_3$, X = Cl, Br, and I): Novel Optoelectronic Materials Showing Bright Emission with Wide Color Gamut. *Nano Letters* **15**(6): 3692-3696, 2015.

[8] Ch. Lu, et al. Cs Oleate Precursor Preparation for Lead Halide Perovskite Nanocrystal Synthesis: The Influence of Excess Oleic Acid on Achieving Solubility, Conversion, and Reproducibility. *Chemistry of Materials* **31**(1): 62-67, 2018.

[9] K. Děcká, et al. On the Role of Cs_4PbBr_6 Phase in the Luminescence Performance of Bright $CsPbBr_3$ Nanocrystals. *Nanomaterials* **11**(8): 1935, 2021.

[10] G. Nedelcu, et al. Fast Anion-Exchange in Highly Luminescent Nanocrystals of Cesium Lead Halide Perovskites ($CsPbX_3$, X = Cl, Br, I). *Nano Letters* **15**(8): 5635-5640, 2015.